JOURNAL OF CATALYSIS **161,** 43–54 (1996)
ARTICLE NO. 0160

Deactivation of Cu/ZSM-5 Catalysts for Lean NO_x Reduction: Characterization of Changes of Cu State and Zeolite Support

J. Y. Yan, G.-D. Lei, W. M. H. Sachtler, and H. H. Kung

V. N. Ipatieff Laboratory, Department of Chemistry, Center for Catalysis and Surface Science, Northwestern University, Evanston, Illinois 60208

Received October 30, 1995; revised January 29, 1996; accepted January 30, 1996

The dependence of the deactivation rate of Cu/ZSM-5 lean NO_x reduction catalysts on the composition of the feed was studied. No catalyst deactivation was observed in the absence of H_2O at 400°C after 160 h. Catalyst deactivation was much faster if the feed contained C_3H_8, NO, O_2, and H_2O (lean NO_x reduction conditions) than if one of these components was missing. Fresh and deactivated catalysts were characterized by a variety of techniques, including EPR, XRD, BET surface area measurements, IR spectroscopy, and temperature programmed reduction with H_2 (H_2-TPR). With some techniques, the differences between fresh and deactivated catalysts were marginal, but very significant changes were observed with TPR and EPR. No gross destruction of the zeolite framework was detected by XRD or BET, even for a catalyst that was 50% deactivated. Isolated Cu^{2+} ions, $[Cu–O–Cu]^{2+}$ oxocations and CuO particles were identified in fresh Cu/ZSM-5. In deactivated Cu/ZSM-5, the Cu species were redistributed. Besides isolated Cu^{2+} ions (in two different coordination environments), highly dispersed Cu ions in Al_2O_3 and a $CuAl_2O_4$ compound were detected. Ion exchange of Cu^{2+} into partially dealuminated H/ZSM-5 yielded TPR and EPR evidence strikingly similar to deactivated Cu/ZSM-5. These results suggested that the formation of proton exchange sites plays a crucial role in catalyst deactivation. In the presence of steam, it induces dealumination of the zeolite, and the copper states are irreversibly changed due to copper interacting with the alumina formed in the dealumination process.

1. INTRODUCTION

Lean-burn engines provide higher fuel efficiency than engines which operate with a stoichiometric air/fuel mixture (1). However, a technical obstacle to large scale introduction of lean-burn engines is that the current three-way exhaust catalyst is unable to destroy NO_x in the engine exhaust in an oxidizing atmosphere (2). This situation has created a strong incentive to develop efficient "lean NO_x" abatement catalysts.

Copper-exchanged ZSM-5 is active for the selective NO_x reduction to N_2 by hydrocarbons, as was first reported by Held *et al.* and Iwamoto *et al.* (3, 4). It is still one of the most active catalysts known to date among a large number of metal/zeolite combinations or mixed oxides (2, 7). However, it is also known that Cu/ZSM-5 catalysts deactivate rapidly under lean-burn conditions (8, 9). Therefore, the objective of the present study is to investigate the deactivation mechanism of these catalysts, in order to provide some guidance to the search for more durable catalysts.

It is widely assumed that copper ions associated with exchange sites of ZSM-5 zeolite are responsible for NO_x reduction activity (see 10, 11, and references cited there). Therefore, deactivation will occur if the state of the Cu ions or the crystal structure of the zeolite is changed. Several reports have been published in which deactivated Cu/ZSM-5 was characterized. Using ^{27}Al NMR, Grinsted *et al.* detected a loss of 23% of framework aluminum after wet-aging a Cu/ZSM-5 catalyst in 10% H_2O/air at 410°C for 113 h (12). The formation of CuO crystallites has been reported by Kharas *et al.* in Cu/ZSM-5-25.5-387 deactivated under simulated lean NO_x condition at 800°C for 1 h (8) and by Tabata *et al.* in a 678% exchanged Cu/ZSM-5 (13), which was consistent with the fact that CuO is ineffective for lean NO_x reduction. However, Matsumoto *et al.* did not detect any CuO crystallites by XRD in a Cu/ZSM-5-20-110 catalyst that had been treated in a simulated lean NO_x mixture at 800°C for 5 h (9). Furthermore, their solid-state NMR results did not indicate serious dealumination of ZSM-5 support. Since the adsorption capacities for NO and CO were drastically lower for the deactivated catalyst, and its electron paramagnetic resonance (EPR) pattern differed from that of fresh Cu/ZSM-5, they concluded that deactivation was mainly caused by migration of Cu^{2+} ions to locations inside ZSM-5 where their reduction to Cu^+ was more difficult.

In the present research, the dependence of the deactivation rate of Cu/ZSM-5 on the composition of the feed was studied. The catalysts were characterized in their active and deactivated states by temperature programmed reduction with hydrogen (H_2-TPR), EPR, XRD, surface area measurement, and IR spectroscopy. The differences in the characteristic parameters of fresh and deactivated catalysts were evaluated in terms of changes in the chemical state of copper and in the structure of the support.

0021-9517/96 $18.00

2. EXPERIMENTAL

2.1. Materials

Cu/ZSM-5 samples were prepared by ion exchange using a solution of $Cu(CH_3COO)_2$ (Aldrich) and Na/ZSM-5 (UOP) (pH 5.5–6) at 25°C, following the method of Iwamoto *et al*. (14). The chemical compositions of the samples were determined by inductive-coupled plasma atomic emission spectroscopy (ICP-AES) with an Atomscan 25 spectrometer (Thermal Jarrel Ash Corp.). The samples are labeled as Cu/ZSM-5-(Si/Al ratio)-(percentage exchange). For samples over 100% exchange, the remaining Na^+ content was small ($Na/Al < 0.03$). All the samples were calcined in O_2 (200 ml/min) at 500°C for 2 h before further treatments. H/ZSM-5 was prepared by calcining NH_4/ZSM-5 at 500°C, which was prepared by exchanging three times Na/ZSM-5 (UOP) with NH_4NO_3 (Fisher). Steam-dealuminated H/ZSM-5 was prepared by steaming H/ZSM-5 in a flow of 10% H_2O/He at 500°C for 11 h. ^{27}Al-NMR results showed that above 60% framework aluminum was removed after the treatment. Cu-exchanged, steam-dealuminated H-ZSM-5(Cu/H-ZSM-5-ST) and Cu/H-ZSM-5 (unsteamed) were prepared under the same conditions using the ion-exchange method described above.

CuO/Na-ZSM-5 was prepared by impregnating a 0.024 *M* $Na_2C_2O_4$ (Johnson–Mathey, ACS grade) solution onto Cu/ZSM-5-18-113 to obtain a $Na/Al = 1.5$. The sample was then calcined in O_2 at different temperatures. XRD showed the formation of CuO crystallites after calcination in O_2 at 500°C for 2 h.

CuO/SiO_2 (1 to 2 wt%) and CuO/Al_2O_3 (1 wt%) were prepared by impregnation of $Cu(NO_3)_2 \cdot 3H_2O$ (Fisher, analytical reagent) on amorphous SiO_2 (Cab-O-Sil) and γ-Al_2O_3 (Alfa, 99.97%, surface area = 100 m^2/g), respectively. The SiO_2-supported sample was then calcined in O_2 at 450°C for 16 h, whereas the Al_2O_3-supported sample was calcined at 500°C for 2 h.

$CuAl_2O_4/Al_2O_3$ (1 wt% Cu) was prepared by calcination of Al_2O_3 impregnated with $Cu(NO_3)_2$ at 825°C in air for 20.5 h, following the method of Hierl *et al.* (15).

Gases (He, O_2, Ar, CO) were ultrahigh purity grade, and C_3H_8/He (1%), O_2/He (25%), NO/He (2%), and H_2/Ar (5%) were custom grade. All gases were used without further treatment, except those used for TPR and IR experiments, which were dried by molecular sieve before use.

2.2. Apparatus and Procedure

A fresh sample of Cu/ZSM-5 was used for each deactivation experiment. In these experiments, the catalysts were treated with two or more of the following gas components: NO (1000 ppm), C_3H_8 (1000 ppm), O_2 (2%), H_2O (10%), balanced with He. H_2O was introduced by flowing He (carrier gas) through a heated water saturator. The standard "wet" catalysis condition refers to the use of a $NO/C_3H_8/O_2/H_2O$/He mixture. However, all catalytic activities reported were evaluated under the standard "dry" catalysis condition using a $NO/O_2/C_3H_8$/He mixture, i.e., without water. The total flow rate was 400 ml/min. Typically, about 100 mg of catalyst was used, which gave a GHSV about 120,000 h^{-1}. The products were analyzed by GC equipped with a Porapak Q and a 5A molecular sieve column. For the data reported,

$$\text{NO conversion}\% = (2N_2/NO_{in}) \times 100\%$$

$$C_3H_8 \text{ conversion}\% = [CO_2/(3C_3H_{8,in})] \times 100\%$$

$$\text{NO competitiveness factor} = [(2N_2)/(10C_3H_{8,consumed})] \times 100\%.$$

The NO competitiveness factor is the percentage of consumed hydrocarbon used for the reduction of NO.

Temperature-programmed reduction was carried out in 5% H_2/Ar (flow rate = 30 ml/min), starting from −48°C with a heating rate of 8°C/min. A thermal conductivity cell was used to monitor the H_2 consumption. The amount of H_2 consumed was calibrated using a physical mixture of $CuO + SiO_2$ as standard. The samples were first calcined in O_2 at 500°C for at least 2 h and cooled in O_2 to −80°C, then purged with Ar (30 ml/min) for 1 h and with H_2/Ar (30 ml/min) for 1 h at −80°C before TPR runs.

Infrared spectra were obtained with a Nicolet 60SX FT-IR spectrometer, using a quartz *in situ* IR cell equipped with NaCl windows and a heater and connected to the heating equipment and a gas manifold. Powder X-ray diffraction data were collected in air with a Rigaku diffractometer. The BET surface areas were measured by N_2 adsorption at 77 K after degassing the samples at 250°C.

Electron paramagnetic resonance data were collected at 77 K with a Varian E-4 spectrometer. After the desired pretreatments, the samples were calcined in O_2 at 500°C for 2 h. After purging the cell with Ar and evacuation at room temperature, the samples were transferred to the EPR sample tubes and sealed under vacuum without exposure to air.

3. RESULTS

3.1. Deactivation of Cu/ZSM-5

The effect of feed composition on deactivation was studied using Cu/ZSM-5-18-113 at 400°C. The catalytic activity was first evaluated using the standard "dry" condition. Then, the catalyst was exposed to different gas mixtures for the time indicated. Afterward, the activity was evaluated again under the standard dry condition. This sequence was repeated until the end of the experiment.

Figures 1A and 1B show the NO and C_3H_8 conversions relative to those of a fresh catalyst after treatments in different feed mixtures for different times. As mentioned earlier,

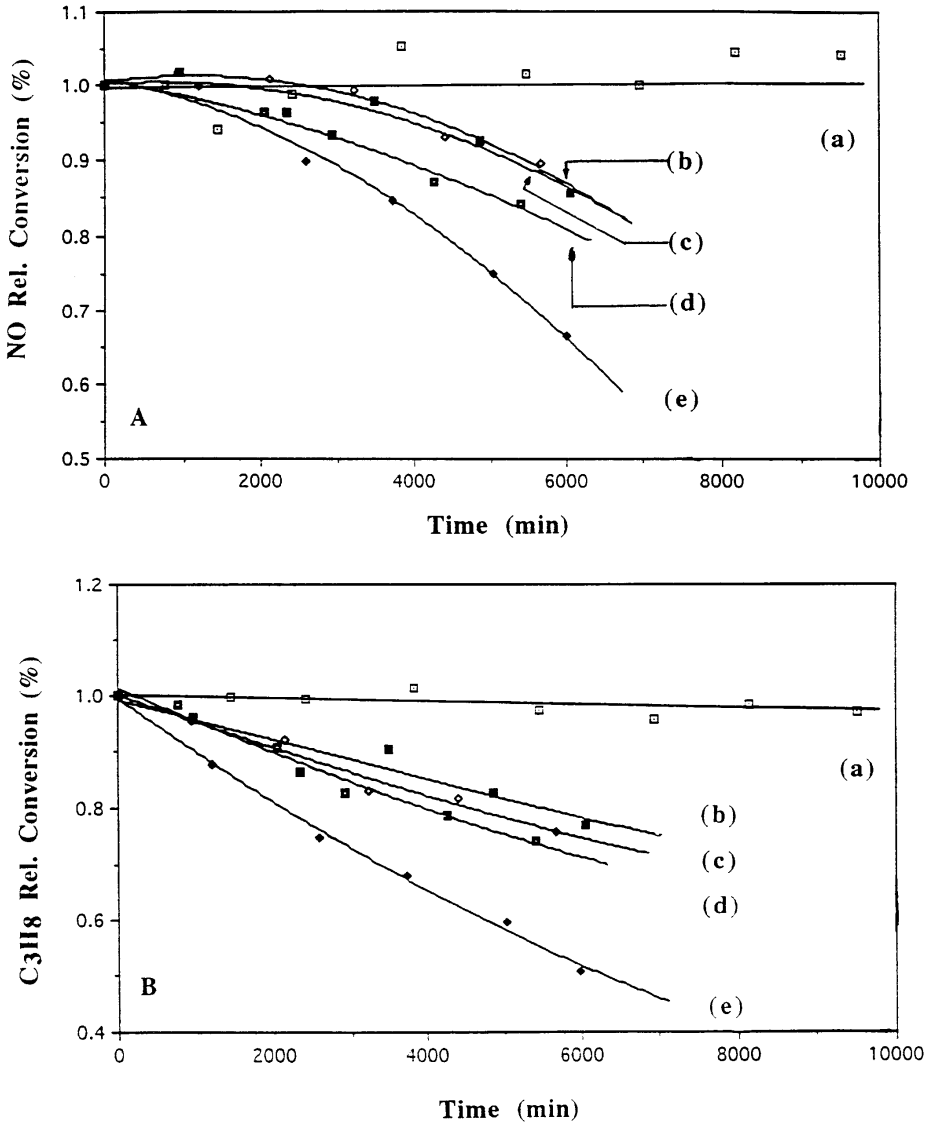

FIG. 1. NO and C_3H_8 conversions (relative to fresh state) of Cu/ZSM-5-18-113 catalyst at 400°C under standard dry catalysis conditions after treatments in different gas mixtures. (a) $NO/C_3H_8/O_2/He$, (b) $NO/O_2/H_2O/He$, (c) $C_3H_8/O_2/H_2O/He$, (d) H_2O/He, and (e) $NO/C_3H_8/O_2/H_2O/He$.

a fresh Cu/ZSM-5-18-113 sample was used for each experiment. The NO and C_3H_8 conversions for these samples were about 60 and 98%, respectively. Treatment of the catalyst by the standard wet condition caused rapid deactivation even at 400°C. The NO conversion dropped to about 2/3, while the propane conversion dropped to about 1/2 of their respective original values after 100 h (curve e). However, exposing the catalyst to the standard dry condition did not cause any deactivation even after 160 h (curve a). The results suggest that H_2O played an important role in the catalyst deactivation, in agreement with literature report (16). To further investigate if the other components in the feed mixture also contributed to deactivation, different Cu/ZSM-5-18-113 samples were treated by water, a mixture of $NO + O_2 + H_2O$, or a mixture of $C_3H_8 + O_2 + H_2O$. The catalytic activities after these treatments are shown by curves b, c, and d in Fig. 1. These results show that deactivation of Cu/ZSM-5 catalyst is much more severe in the presence of all components in the reaction mixture than if one component is absent.

The NO competitiveness factor also decreased during deactivation, as shown in Fig. 2. This suggests that not only were there fewer active sites in the deactivated catalyst, but the properties of the active sites had changed also.

3.2. Temperature Programmed Reduction

Fresh and deactivated catalysts were characterized by a variety of methods. Many techniques showed only small differences between fresh and deactivated samples. In

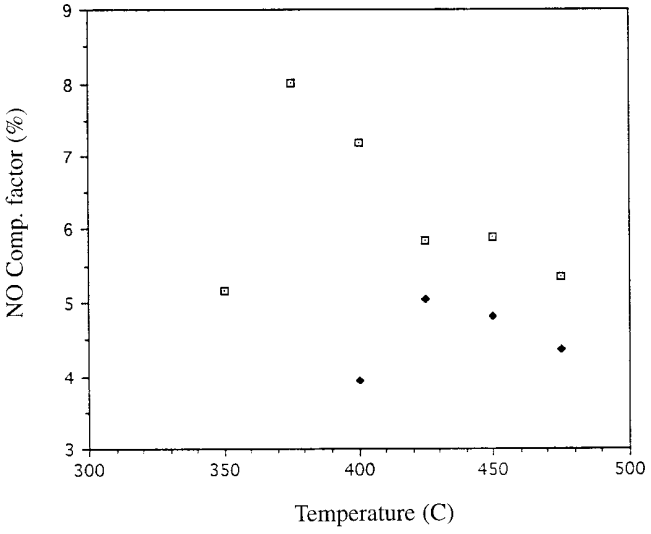

FIG. 2. NO competitiveness factor of Cu/ZSM-5-18-113 before and after deactivation. Open squares, fresh sample; filled diamonds, after 77 h treatment in standard wet catalysis condition.

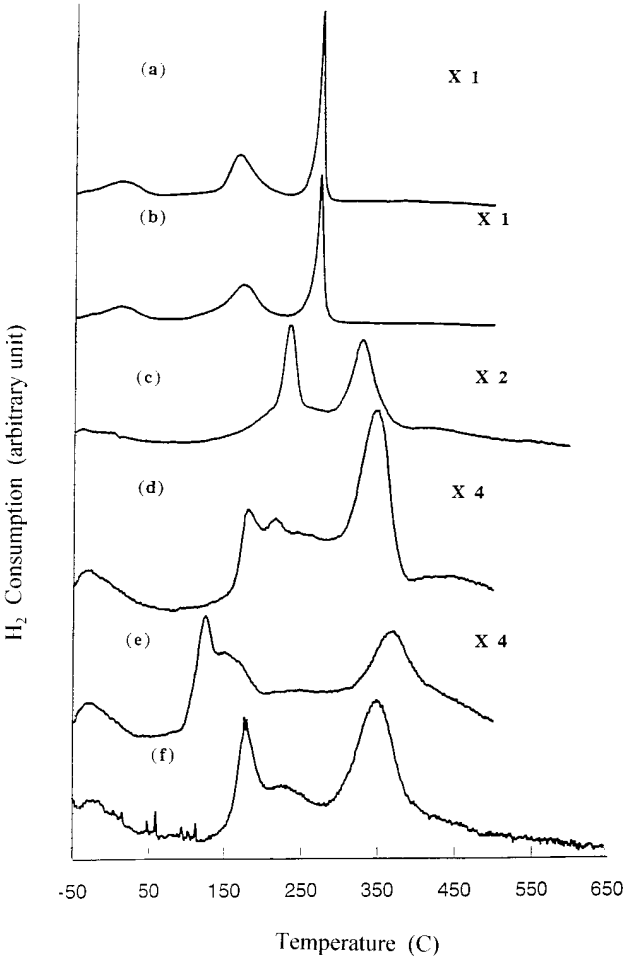

FIG. 3. H_2-TPR profiles of (a) fresh Cu/ZSM-5-18-113, (b) fresh Cu/ZSM-5-18-113 after a reduction and reoxidation treatment, (c) Cu/ZSM-5-18-113 after treatment under the standard wet catalysis condition for 19.5 h, (d) Cu/ZSM-5-18-113 after treatment under the standard wet catalysis condition for 44 h, (e) after (d) and reoxidized in O_2 at 500°C for 2 h, and (f) Cu/ZSM-5-ST-17-86.

contrast, H_2-TPR revealed marked, reproducible differences between fresh and deactivated catalysts. Therefore, much emphasis was placed on the TPR data and their interpretation.

3.2.1. TPR of fresh Cu/ZSM-5. A H_2-TPR profile of the fresh, calcined Cu/ZSM-5-18-113 is shown by curve a in Fig. 3. There were three H_2 consumption peaks centered at about 15, 165, and 275°C. Their relative areas were 10, 43, and 47%, respectively. The 275°C reduction peak was unusually narrow and asymmetric in shape. The ratio of total hydrogen consumption to copper was unity ($H_2/Cu = 1$), indicating that most of the copper was in the +2 valance state before TPR, and the reduction of copper was complete after TPR. The signal below 0°C was not due to H_2 consumption but to Ar desorption, leading to dilution of the H_2 in the gas stream.

3.2.2. TPR of deactivated Cu/ZSM-5. Two TPR profiles of Cu/ZSM-5-18-113 deactivated by catalytic treatment under the standard wet condition at 500°C for 19.5 and 44 h are shown by curves c and d in Fig. 3, respectively. The activities of these samples at 400°C after the treatments are listed in Table 1. Compared to the fresh sample, these TPR profiles showed the following changes: (a) The peak at 15°C almost disappeared. (b) In the region of 100–400°C, a broad reduction signal appeared with a maximum at around 250°C. This suggests that some new copper species were formed during catalyst deactivation. The reduction peak at 165°C was no longer clearly distinguishable. (c) The high temperature peak shifted from 275°C to higher temperatures and became broader, and the intensity also decreased. (d) A small new reduction peak appeared at an even higher temperature, around 430–450°C, and was more prominent for the highly deactivated sample (curve d). (e) The H_2/Cu ratio for curve 3c was 1, but was 0.92 for curve d.

3.2.3. Differentiation between reversible and irreversible changes. To test whether the Cu species could be reversibly reduced and reoxidized, a fresh sample was first reduced in a H_2-TPR experiment up to 500°C, calcined in O_2 at 500°C for 2 h, and then reduced again in H_2-TPR. The profile of the second reduction (curve b in Fig. 3) was very similar to that of curve a. This suggests that the Cu^0 formed in the first TPR could be reoxidized and the resulting oxide underwent protonolysis to Cu^{2+} ions that were positioned back into the original sites. Under these conditions, the reduction–oxidation cycle did not cause obvious permanent changes of the sample.

However, irreversible changes were detected in the deactivated samples. When a highly deactivated Cu/ZSM-5-

TABLE 1

Lean NO_x Reduction Activities and Ionic Copper Distributions in Fresh and Deactivated Cu/ZSM-5[a,b]

NO conv. relative to fresh catalyst	C_3H_8 Conv. relative to fresh catalyst	$[Cu–O–Cu]^{2+}$ (%)	Cu^{2+c} (%)	Total nonoxide copper ion (%)[d]	Pretreatment	Specific surface area (m^2/g)
1.0	1.0	19	75	94	Fresh calcined	262
1.0	1.0	18	79	96	Standard dry condition, 400°C, 3 h	—
—	0.9	8	82	90	Calcined in O_2 100 h	—
1.0	0.91	0	84	84	Standard dry condition, 500°C, 91 h	—
0.75	0.46	0	70	71	Standard wet condition, 500°C, 19.5 h	—
0.49	0.37	0	64	64	Standard wet condition, 500°C, 44 h	296
0.39	0.25	0	49	49	Standard wet condition, 500°C, 19 h/TPR/recalcined/standard wet condition, 500°C, 19 h	299
0.37	0.28	0	37	37	Copper exchanged steam-dealuminated H/ZSM-5-17	—

[a] Catalytic activities were evaluated at 400°C under the standard dry condition and compared with fresh Cu/ZSM-5-18-113 sample.
[b] Ionic copper distribution was calculated from H_2-TPR results.
[c] Isolated Cu^{2+} species.
[d] Sum of $[Cu–O–Cu]^{2+}$ and Cu^{2+}.

18-113 sample, which had been reduced in TPR to 500°C (curve d in Fig. 3), was calcined in O_2 at 500°C for 2 h and then reduced again in H_2-TPR, the profile shown by curve e in Fig. 3 was obtained. It shows a new reduction feature at 130°C.

3.2.4. TPR of CuO/Na-ZSM-5, CuO/SiO_2, CuO/Al_2O_3, and $CuAl_2O_4$/Al_2O_3. In order to identify the different copper species in a fresh and a deactivated Cu/ZSM-5, H_2-TPR was performed with several supported CuO samples. Curve a in Fig. 4 shows the TPR profiles of CuO/Na-ZSM-5. The ratio of H_2/Cu was 1. The XRD spectrum of this sample confirmed the formation of CuO crystallites without obvious loss of zeolite crystallinity (curve c in Fig. 6). Table 2 shows the reduction peak temperatures of CuO/Na-ZSM-5 that were calcined at different temperatures to change the particle size of CuO. These data show that CuO crystallites on ZSM-5 were reduced below 200°C.

The H_2-TPR profile of CuO/SiO_2 is shown by curve b in Fig. 4. There was a sharp H_2 consumption peak at about 200°C, in agreement with the literature results (17), and a small peak above 300°C, which might be due to the reduction of a copper compound formed by interaction of CuO with contaminants on SiO_2 during calcination.

The profile of CuO/Al_2O_3 is shown by curve c in Fig. 4. It showed a sharp peak at 130°C, which had an area that corresponded to reduction of only 10% of the total copper in the sample. Comparison with other samples suggests that this peak was due to the reduction of CuO crystallites. There was a broad reduction peak over the range from 100 to 500°C with a maximum at around 250°C. Complete reduction of copper was achieved at the end of the TPR experiment.

The profile of $CuAl_2O_4$/Al_2O_3 is shown by curve d in Fig. 4. Unlike the other profiles, no sharp reduction peak was observed. Instead, there was a very broad peak with a maximum at about 400°C. Reduction of copper was incomplete even at 700°C; i.e., reduction of $CuAl_2O_4$ was slow.

3.2.5. TPR of Cu-exchanged steam-dealuminated H-ZSM-5 (Cu/H-ZSM-5-ST). In order to check our interpretation of the TPR results, Cu^{2+} was exchanged into a H/ZSM-5-17 sample that was first steam-dealuminated in 10% H_2O at 500°C for 11 h. ^{27}Al-NMR showed that the dealuminated H/ZSM-5 had lost 60% of the framework aluminum. The sample also showed a loss of exchange capacity (116% nominal copper exchange level for unsteamed and 86% for steamed H/ZSM-5). The TPR profile of Cu/H-ZSM-5-ST-17-86 is shown by curve f in Fig. 3. It was similar to that of highly deactivated Cu/ZSM-5-18-113 (curve d), except for the absence of the high temperature (>400°C) peak and a more predominant peak at 175°C.

3.3. FTIR of CO Adsorption on Cu/ZSM-5

The reduction of Cu^{2+} to Cu^+ was followed by adsorption of CO on Cu^+ using FT-IR. The results are shown in Fig. 5. A fresh Cu/ZSM-5-17-102, after calcination in O_2 at 450°C for 2 h, was cooled to 30°C in O_2 and then purged with He for 1h. The sample showed no IR band in the range of 2000–2300 cm^{-1} (Fig. 5a). After exposing it to a flow of pure CO at 30°C for 20 min and then He for 20 min, spectrum 5b was collected. Two bands appeared at 2157 and 2176 cm^{-1}, which had been assigned to Cu^+–CO and Cu^+–$(CO)_2$, respectively (18). The second band of the dicarbonyl species at 2150 cm^{-1} overlapped with the Cu^+–CO band. The sample was then heated at 200°C in a flow of 30% H_2 in He for 10 min. After cooling to 30°C in He, the sample was again exposed to CO for 20 min and purged with He for

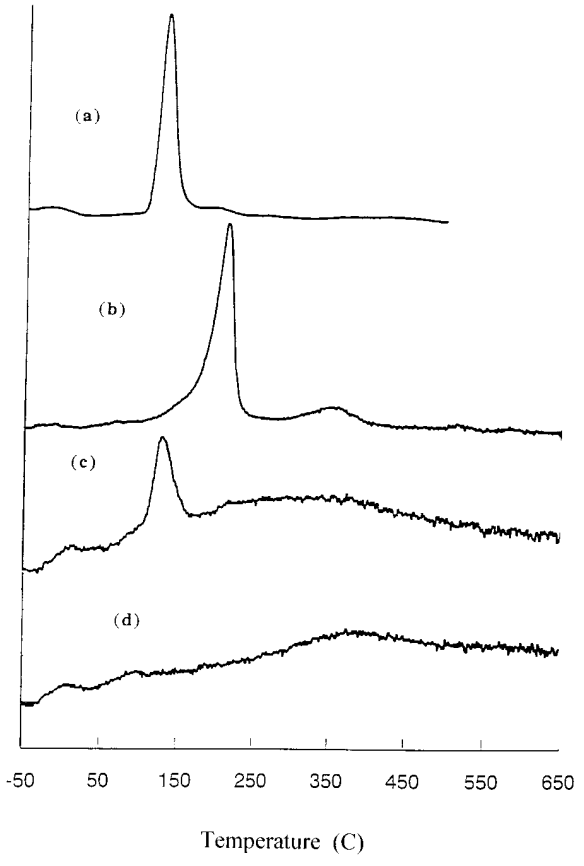

FIG. 4. H_2-TPR profiles of (a) CuO/Na-ZSM-5, (b) 2 wt% CuO/SiO_2, (c) 1 wt% CuO/Al_2O_3, and (d) 1 wt% $CuAl_2O_4$.

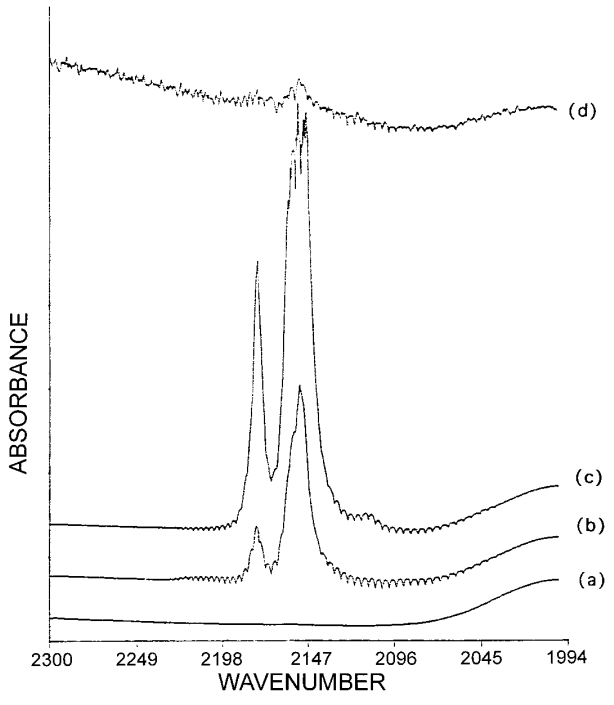

FIG. 5. IR spectra of Cu/ZSM-5-17-102 after H_2 reduction and CO adsorption. (a) After calcination in O_2 and purged with He, (b) after (a) and CO adsorption at 30°C, (c) after (b) and H_2 reduction at 200°C and CO adsorption at 30°C, (d) after (c) and H_2 reduction at 400°C and CO adsorption at 30°C.

20 min. Spectrum 5c was then recorded. The IR bands of the Cu^+–CO and Cu^+–$(CO)_2$ species became very intense. The relative intensity ratio (calculated by using the height at the half peak width of the 2176 cm^{-1} peak) of Cu^+–$(CO)_2$ in spectra b and c was 1 : 4. Further reduction with H_2 at 400°C resulted in spectrum 5d. The IR signals became very weak, and the sample color changed to reddish, indicating formation of metallic copper.

3.4. XRD and Surface Area

XRD patterns of the fresh and deactivated Cu/ZSM-5 are shown by curves a and b in Fig. 6. Comparison of these two spectra suggests that there was no obvious loss of zeolite crystallinity after deactivation, in agreement with literature results (9). In addition, the pattern of deactivated Cu/ZSM-5 did not show the formation of detectable CuO Crystallites ($d > 4$ nm).

The pattern of Cu^0/ZSM-5 (which was prepared by H_2-TPr of Cu/ZSM-5 to 500°C) is shown by curve c in Fig. 6. It showed formation of large copper metal particles ($2\theta = 43.55°$). Since XRD did not show any obvious loss of zeolite crystallinity, the copper metal particles might have been formed on the external surface of the zeolite particles. The pattern of CuO/Na-ZSM-5 is shown by curve d in Fig. 6. It showed CuO peaks at 35.7° and 38.55° 2θ.

The BET surface areas of several fresh and deactivated Cu/ZSM-5 samples are listed in Table 1. No loss of surface area caused by deactivation was detected. Thus, neither XRD nor surface area suggests significant degradation of the zeolite structure by deactivation.

TABLE 2

CuO/Na-ZSM-5 Calcination Temperature and T_{max} in H_2-TPR

Calcination temperature (C)	200	300	400	500	600	700
T_{max} (C)	158	151	147	130	147	154

Note. Samples were calcined in UHP O_2 at certain temperature for 2 h.

3.5. Electron Paramagnetic Resonance

Figure 7 shows the EPR spectra of fresh (curve a) and deactivated (curve b) Cu/ZSM-5-18-113. The deactivated sample showed features not present in the fresh sample. In particular, there was a broad feature at about 3000 G that was similar to that found in CuO/Al_2O_3 after calcination in O_2 at 700°C for 5 h (curve c in Fig. 7). The hyperfine structures in these spectra are shown in Fig. 8. The spectrum of

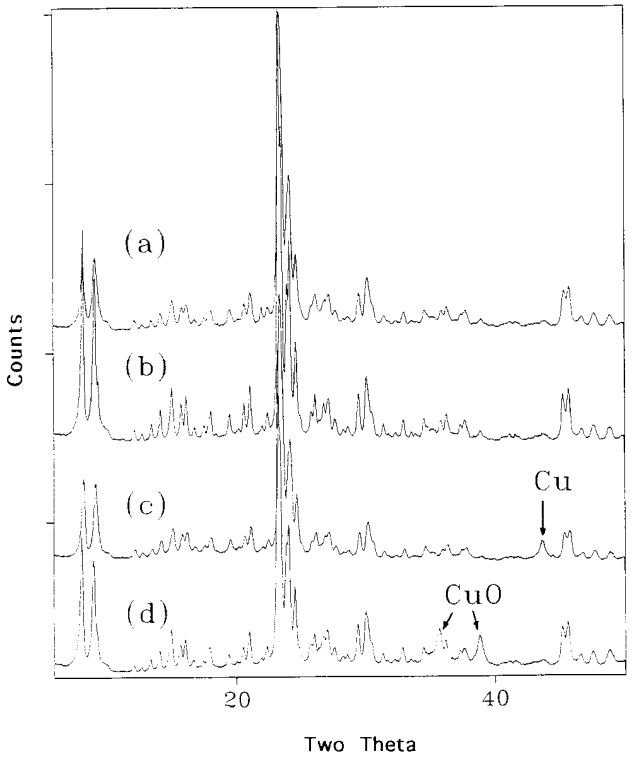

FIG. 6. XRD spectra of (a) fresh Cu/ZSM-5-18-113, (b) deactivated Cu/ZSM-5-18-113 after treatment under the standard wet catalysis condition for 44 h, (c) Cu/ZSM-5-18-113 after H_2-TPR to 500°C, (d) CuO/Na-ZSM-5-18-113.

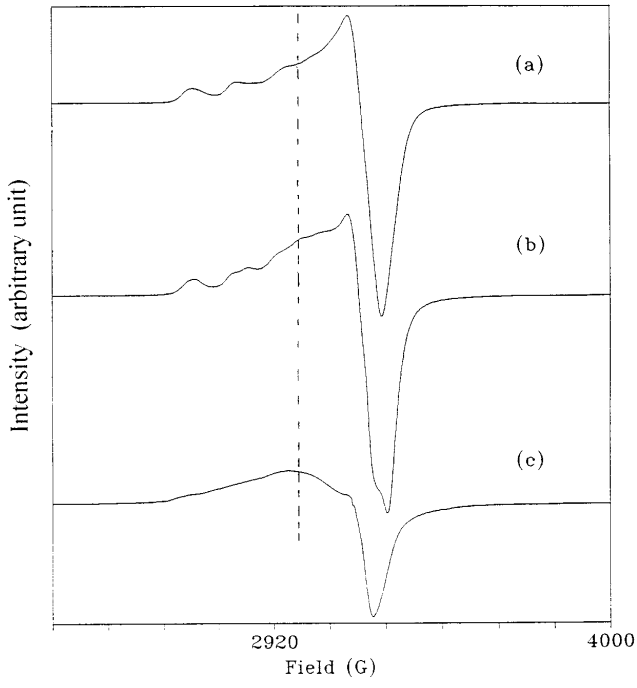

FIG. 7. EPR spectra of (a) fresh Cu/ZSM-5-18-113, (b) deactivated Cu/ZSM-5-18-113 after treatment under the standard wet catalysis condition for 44 h, (c) Cu/Al_2O_3 after calcination in O_2 at 700°C for 5 h.

the fresh sample could be assigned to only one Cu^{2+} species with $A_\parallel = 154$ G and $g_\parallel = 2.30$. In the deactivated sample (spectrum 8b), two Cu^{2+} species can be discerned, one of which, with $A_\parallel = 148$ G and $g_\parallel = 2.31$, was likely the same species as that detected in the fresh sample. The new species had $A_\parallel = 174$ G and $g_\parallel = 2.26$. These results indicated that deactivation induced migration of some Cu^{2+} ions to sites with different coordination environments.

The EPR spectra of copper-exchanged, unsteamed and steamed H-ZSM-5-17 are shown in Figs. 9a and 9b, and their hyperfine structures in Figs. 10a and 10b, respectively. They showed that one Cu^{2+} species was present in Cu/H-ZSM-5-17-116 (unsteamed sample), but two Cu^{2+} species in Cu/H-ZSM-5-ST-17-86.

Table 3 lists the relative concentrations of EPR active Cu^{2+} measured by the intensity of the EPR signals for the fresh and deactivated Cu/ZSM-5, CuO/ZSM-5, CuO/Al_2O_3, CuO/SiO_2, and $CuO + SiO_2$ (physical mixture), as well as Cu/ZSM-5 after H_2-TPR to 240 and 450°C.

4. DISCUSSION

The results described above show the following characteristics regarding the deactivation of a slightly overexchanged Cu/ZSM-5 catalyst:

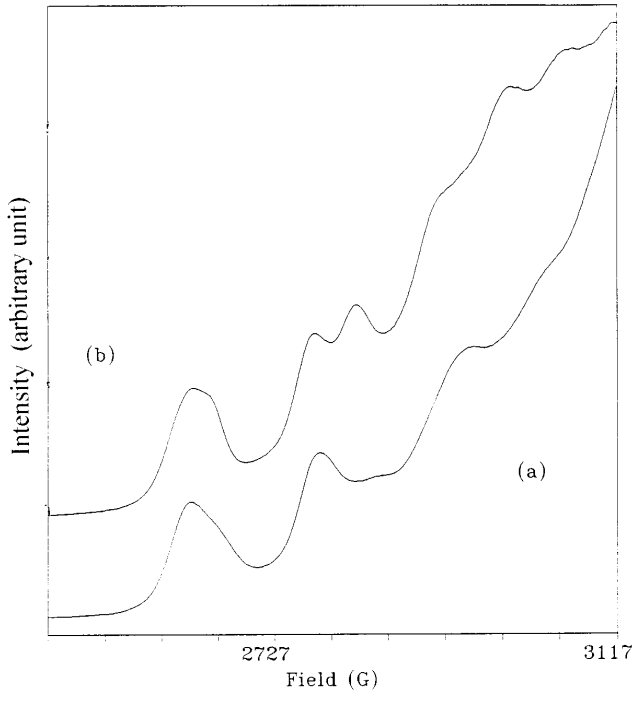

FIG. 8. EPR spectra of copper hyperfine structures of (a) fresh Cu/ZSM-5-18-113, (b) deactivated Cu/ZSM-5-18-113 after treatment under the standard wet catalysis condition for 44 h.

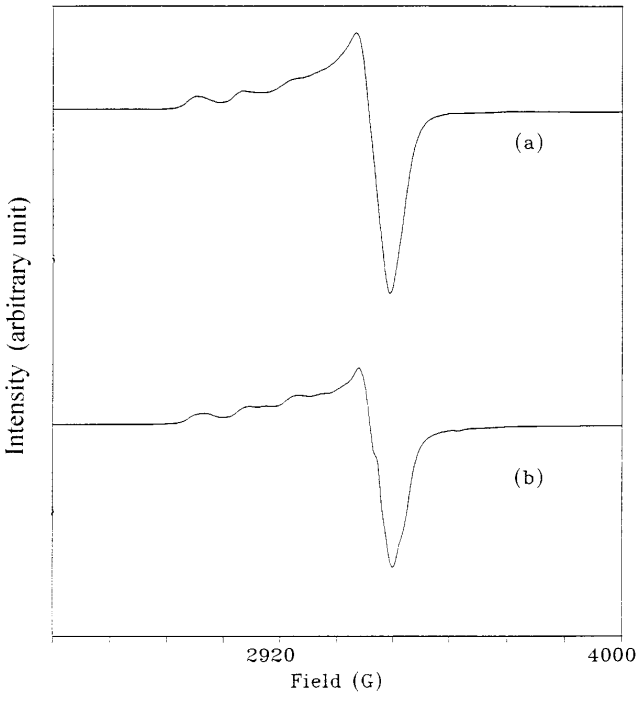

FIG. 9. EPR spectra of (a) Cu/H-ZSM-5-17-116 (unsteamed) and (b) Cu/H-ZSM-5-ST-17-86.

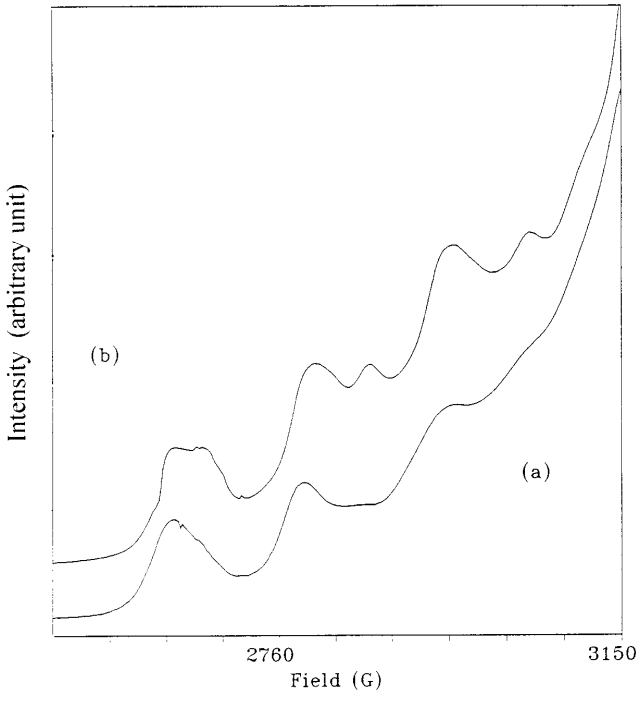

FIG. 10. EPR spectra of copper hyperfine structures of (a) Cu/H-ZSM-5-17-116 (unsteamed) and (b) Cu/ H-ZSM-5-ST-17-86.

TABLE 3

EPR Intensities of Some Copper Containing Samples

Sample[a]	Cu wt%	EPR relative intensity/Cu[b]
Cu^0/ZSM-5 (after H_2-TPR to 450°C)	2.8	N/D[c]
Fresh calcined Cu/ZSM-5H_2-TPR to 240°C	2.8	0.2 (0.04)
Fresh calcined Cu/ZSM-5	2.8	1.0 (0.2)
Deactivated Cu/ZSM-5 after 43 h wet catalysis at 500°C and recalcination	2.8	1.5 (0.3)
Copper exchanged steamed H/ZSM-5	2.0	1.1 (0.2)
$CuO + SiO_2$	2.0	N/D[c]
CuO/SiO_2 calcined in O_2 at 700°C, 1.5 h	1.0	0.2 (0.04)
CuO/H-ZSM-5	2.8	0.2 (0.03)
CuO/Al_2O_3 calcined in O_2 at 700°C, 5 h	1.0	2.2 (0.4)

[a] All the samples were prepared in vacuum and sealed in EPR tubes after pretreatment, except that CuO/SiO_2, CuO/H-ZSM-5, and $CuO + SiO_2$ were prepared in air.

[b] The intensities of isolated Cu^{2+} in EPR were calculated by double integration of the spectra and ratioed to the fresh Cu/ZSM-5-18-113. The number in parentheses is the relative experimental error.

[c] N/D, not detectable.

(1) Deactivation is significant when the catalyst is exposed to a gas mixture containing water vapor at the reaction temperature. The deactivation rate is faster if the feed contains C_3H_8, NO, O_2, and H_2O than if one of these components is lacking. No deactivation is observed in the absence of water.

(2) New copper species are detected in the deactivated catalyst, giving rise to new TPR and EPR features.

(3) No gross destruction of the zeolite framework is detected by XRD, and little change is found in surface areas.

An interpretation of these observed changes of the state of copper and the zeolite during deactivation is as follows.

4.1. Copper Species in Cu/ZSM-5

4.1.1. Copper species in fresh Cu/ZSM-5. An oxygen bridged oxocation $[Cu–O–Cu]^{2+}$ has been proposed to exist in Cu/ZSM-5 (13, 19, 20). Sometimes, the bridging oxygen ion is referred to as "extra-lattice oxygen," or ELA (21). The oxocation is easily reducible by removal of the bridging oxygen. In the TPR profile of fresh Cu/ZSM-5-18-113, the first reduction peak (at 15°C in curve a of Fig. 3) has been assigned to this reduction (19):

$$[Cu–O–Cu]^{2+} + H_2 \Longrightarrow 2Cu^+ + H_2O. \qquad [1]$$

The IR results support this assignment. Exposure of the sample to CO at 30°C results in the formation of Cu^+–CO (2157 cm^{-1}) and Cu^+–$(CO)_2$ (2176 cm^{-1}), which are likely formed by

$$[Cu–O–Cu]^{2+} + 3CO \Longrightarrow 2Cu^+–CO + CO_2 \qquad [2]$$

$$Cu^+–CO + CO \Longrightarrow Cu^+–(CO)_2. \qquad [3]$$

In Cu/ZSM-5 prepared by ion-exchange, isolated Cu^{2+} ions will, of course, prevail. The oxocations, $[Cu–O–Cu]^{2+}$, can be visualized as resulting from partial hydrolysis of the Cu^{2+} ions:

$$2Cu^{2+} + H_2O \Longrightarrow [Cu–O–Cu]^{2+} + 2H^+. \quad [4]$$

Likewise, hydrolysis can lead to Cu hydroxide oligomer which, upon calcination, is transformed to CuO particles.

A stepwise reduction mechanism for Cu^{2+} to Cu^0 in the Cu–Y system has been proposed and systematically studied (22, 23). The first detectable products of the reduction of Cu^{2+} ions with H_2 are Cu^+ ions and protons. After Cu^{2+} are reduced to Cu^+, further reduction with H_2 leads to Cu^0. This reduction mechanism is consistent with the present data for Cu/ZSM-5. Thus, the second and third reduction peaks in the TPR profile of fresh Cu/ZSM-5-18-113 (curve a, Fig. 3) can be assigned to the two stages of the reduction of Cu^{2+} to Cu^0,

$$Cu^{2+} + 1/2H_2 \Longrightarrow Cu^+ + H^+ \quad [5]$$

$$Cu^+ + 1/2H_2 \Longrightarrow Cu^0 + H^+. \quad [6]$$

This assignment suggests that Cu^+ ions are created when the sample is reduced to 200°C, i.e., between the second and third reduction peaks. This is confirmed by the IR spectrum of the sample after reduction in H_2 at 200°C, which shows intense bands of Cu^+–CO and Cu^+–$(CO)_2$ (spectrum 5c). Upon reducing the sample in H_2 to 400°C, most of the Cu^+ is reduced to Cu^0.

The EPR data also support the stepwise reduction mechanism (Table 3). The intensity of isolated Cu^{2+} decreased more than 80% after the sample was reduced by H_2 to 240°C. After reduction to 450°C, no detectable Cu^{2+} was left.

Although Cu^{2+} ions are expected to be located in exchange sites in zeolite samples prepared by ion-exchange in an acidic solution (pH < 6), some imbibed copper acetate could remain in the zeolite, unless the sample is thoroughly washed with H_2O after the exchange. Decomposition of this copper acetate will lead to formation of CuO particles. Another possible cause for the presence of CuO is the equilibration between CuO and $Cu^{2+}/[AlO_2^-]_2$,

$$Cu^{2+}/[AlO_2^-]_2 + H_2O = CuO + 2H^+/[AlO_2^-], \quad [7]$$

or a similar equilibration among Cu^{2+}, $[Cu–O–Cu]^{2+}$, and CuO, which is controlled by the distribution of exchange sites and the water content (Eqs. [4], [7], and [8]):

$$2Cu^{2+}/[AlO_2^-]_2 + H_2O = [Cu–O–Cu]^{2+}/[AlO_2^-]_2 + 2H^+/[AlO_2]. \quad [8]$$

CuO particles in Cu/ZSM-5 samples have been identified by Sárkány *et al.* using CO-TPR (19) and by Beutel *et al.* using NO as the probe molecule in IR spectroscopy (24). They can be reduced at 130–160°C, as shown by TPR of CuO/Na-ZSM-5 (Table 2). The slight increase in the baseline between 100 and 200°C in the profile of fresh Cu/ZSM-5 TPR (curve a, Fig. 3) may be due to this reduction.

The relative concentrations of the three major copper species in fresh Cu/ZSM-5 can be calculated as follows:

$$(\text{area of } 15°\text{C peak}) \times 2 = H_2 \text{ consumption for reduction of } [Cu–O–Cu]^{2+} \text{ to } 2Cu^0 \quad [9]$$

$$[(\text{area of } 275°\text{C peak}) - (\text{area of } 15°\text{C peak})] \times 2 = H_2 \text{ consumption for the reduction of isolated } Cu^{2+} \text{ to } Cu^0. \quad [10]$$

The remaining H_2 consumption is due to the reduction of CuO to Cu^0. For Cu/ZSM-5-18-113, the relative concentrations are $[Cu–O–Cu]^{2+}$ (19%), Cu^{2+} (75%), and CuO (6%).

From the IR peak intensities, the ratio of the Cu^+ concentrations (detected as Cu^+–$(CO)_2$ by exposure to CO at 30°C) that are generated by: (a) CO reduction of $[Cu–O–Cu]^{2+}$ at 30°C (Eq. [2]) or (b) H_2 reduction up to 200°C of $[Cu–O–Cu]^{2+}$ and Cu^{2+} ions (Eqs. [1] and [5]) can be estimated. This ratio, $Cu^+_{(a)}/Cu^+_{(b)} = 1:4$, is close to the 1 : 5 ratio of $[Cu–O–Cu]^{2+}$ to total (Cu^{2+} + $[Cu–O–Cu]^{2+}$) content calculated from the TPR results.

It is interesting that the 275°C peak has a sharp drop on the high temperature side, indicating an autocatalytic process. One possibility is that Cu^0 atoms, which interact weakly with the zeolite framework, migrate and coalesce to form Cu^0 clusters, as has been found with other zeolite-supported transition metals (25, 26). As H_2 is dissociatively adsorbed on Cu metal surfaces, their presence will enhance further reduction of the Cu^+. The extent of such an autocatalytic process should depend on the concentration of Cu^0 particles. Indeed, this high temperature peak for a lower loading Cu/ZSM-5-17-102 sample appears at a higher temperature of 298°C, and the peak is neither as narrow nor as skewed. This is consistent with the model: the contribution to the reduction process by the migration Cu^0 is less due to a lower copper coverage.

4.1.2. Copper species in deactivated Cu/ZSM-5. The TPR profiles of deactivated Cu/ZSM-5 (curves c and d in Fig. 3) indicate the presence of a number of new copper species. By comparing the reduction temperatures and peak shapes of highly deactivated Cu/ZSM-18-113 (curve d in Fig. 3) with those of $CuAl_2O_4/Al_2O_3$ (curve d in Fig. 4), it appears that the TPR peak above 400°C in deactivated Cu/ZSM-5 is similar to the reduction of $CuAl_2O_4$. Therefore, this new copper species is assigned to $CuAl_2O_4$.

The broad peak in the range of 100–400°C contains multiple copper species, because its shape differs for samples de-

activated to different extent. Comparison of this peak with the reduction peaks of CuO/SiO_2, CuO/Al_2O_3, CuO/Na-ZSM-5, and Cu/H-ZSM-5-ST suggests assignments to various copper species. CuO crystallites supported on Na-ZSM-5, SiO_2, or Al_2O_3 are reduced between 100 and 250°C in a single peak (Figs. 4a, 4b, and 4c). The variation in the peak position may be due to different crystallite sizes, as well as different interaction with different supports. A broad feature is observed for the Cu/Al_2O_3 sample that is not found on SiO_2 or Na/ZSM-5 supported samples. There is evidence that this broad feature is also present on the deactivated sample, and it is more apparent for the less deactivated sample (Fig. 3c). This suggests that at least some of the new copper species formed are associated with Al_2O_3, in the form such as copper ions dispersed in Al_2O_3, but not CuO crystallites.

Of particular interest is the TPR profile of copper ion-exchanged into steam-dealuminated H-ZSM-5 (Fig. 3, curve f). This pattern appears to be intermediate between those of the two deactivated samples (Fig. 3, curves c and d) in that the broad peak between 100 and 400°C is intermediate in intensity, and the peak at the low temperature edge of this broad peak is intermediate in intensity and in temperature. The only difference is that in the highly deactivated sample (Fig. 3, curve d), there is also a small broad peak at 430°C, which indicates the formation of $CuAl_2O_4$ compound. This is consistent with the fact that $CuAl_2O_4$ is formed in CuO/Al_2O_3 only after prolonged heating at high temperatures.

These results suggest that the appearance of this new group of copper species is associated with the dealumination process of the zeolite support. The following model is proposed to explain these results. At the early stage of deactivation, dealumination of the zeolite sample occurs, as evidence by the increase in the H_2 consumption in TPR between 100 and 400°C. Simultaneously, formation of small CuO crystallites occurs, which are situated primarily on the silicious portion of the zeolite. As deactivation and dealumination become more severe, there are increasingly more Al_2O_3 particles formed, as well as small CuO clusters on Al_2O_3, Cu^{2+} on Al_2O_3, and some copper ions that have reacted with Al_2O_3 to form $CuAl_2O_4$ compound, in addition to the remaining Cu^{2+} ions on the exchange sites of ZSM-5, and CuO on silicious portion of zeolite.

Since the TPR profiles of CuO crystallites on various supports show a peak only in the range of 100–250°C, the high temperature reduction peak (>300°C) in the profile of deactivated Cu/ZSM-5 must be due to another copper species. Based on the previous discussion on TPR of fresh Cu/ZSM-5, it is reasonable to assume that this peak is due to reduction of isolated Cu^+ to Cu^0, similar to the 275°C peak of the fresh Cu/ZSM-5 profile. With this assumption, it is possible to estimate the total isolated Cu^{2+} ions on exchange sites using Eq. [10]. The percentages of isolated Cu^{2+} in Cu/ZSM-5 samples deactivated to different extents are listed in Table 1. This percentage decreases with increasing severity of deactivation.

Kharas *et al*. observed the formation of CuO crystallites and degradation of ZSM-5 structure in their deactivated samples with very high copper loading (378% of nominal exchange level) (8). They suggested that catalyst deactivation is caused by agglomeration of Cu^{2+} ions to inactive CuO, and local collapse of the zeolite lattice induced by growing CuO crystallites inside the zeolite channels. Likewise, Tabata *et al*. also reported the formation of CuO (13). In the present work, the copper loading was much lower (113% nominal exchange level) and the samples were deactivated at relative low temperatures (400–500°C). No obvious change of zeolite crystallinity was detected by XRD. Since the Cu^{2+} ions in CuO crystallites are not detectable by EPR because of the strong antiferromagnetic coupling, agglomeration to CuO should result in a decrease of the EPR intensity. In reality, the EPR intensity of Cu^{2+} for the deactivated samples is higher than that in the fresh sample (Table 3). This shows that some of the originally EPR-silent species, such as $[Cu–O–Cu]^{2+}$ have become EPR active, and more importantly, agglomeration to CuO crystallites is not the major cause of catalyst deactivation in samples that have lost almost 51% of their original activities. One possibility is that these Cu^{2+} ions are highly dispersed on or in the Al_2O_3 that is formed by the dealumination of the zeolite. They would be EPR active. In support of this hypothesis, Table 3 shows that CuO supported on SiO_2 or ZSM-5 gives very weak EPR signals, but when supported on Al_2O_3, a strong EPR signal of Cu^{2+} is detected. Furthermore, the shapes of the EPR signals of Cu/Al_2O_3 and deactivated Cu/ZSM-5 show some similarities (broad feature around 3000 G in Fig. 7, spectra b and c), Thus, these EPR and TPR results suggest that in a deactivated Cu/ZSM-5 catalyst, some Cu^{2+} ions have migrated onto Al_2O_3 and remain highly dispersed on Al_2O_3. Copper in this state is inactive toward NO_x reduction. (An independent experiment showed that Cu/Al_2O_3 has no NO reduction activity under the standard dry condition.) In addition, Cu ions in $CuAl_2O_4$ could also contribute to the EPR signal in the deactivated catalyst.

4.2. *Change of Cu^{2+} Coordination*

As mentioned earlier, the decrease of competitiveness factors due to deactivation suggests changes in the catalytic properties of some of the copper species. In Table 1, it is shown that the concentration of isolated Cu^{2+} ions on exchange sites decreases at a lower rate than the NO conversion. Thus, some of the Cu^{2+} ions become less active or inactive. These data suggest changes in the coordination environment of the Cu^{2+} ions at exchange sites in the deactivated sample. This is consistent with the fact that the EPR spectra (Fig. 8) show new Cu^{2+} species formed that have different hyperfine splitting.

A clue as to the cause of the migration of Cu^{2+} ions to different coordination environments is provided by comparing the EPR spectra of samples that were prepared by exchanging Cu^{2+} ions into either unsteamed or steamed H/ZSM-5 (Figs. 9 and 10). The EPR spectrum of Cu/H-ZSM-5-17-116 (unsteamed) shows only one signal for isolated Cu^{2+} ions (curve a in Fig. 10), but the spectrum of Cu/H-ZSM-5-ST-17-86 shows the presence of at least two isolated Cu^{2+} species (curve b in Fig. 10). Remarkably, the hyperfine region of the Cu/H-ZSM-5-ST spectrum is similar to that of deactivated Cu/ZSM-5-18-113 (Fig. 8b). This suggests that the appearance of the second isolated Cu^{2+} ion upon deactivation is accompanied by some dealumination of the ZSM-5 support.

It is worth mentioning that both types of Cu^{2+} ions in the deactivated sample are still accessible to small molecules, such as H_2O. When the deactivated Cu/ZSM-5 sample was exposed to air, the EPR spectrum showed only one type of Cu^{2+} ions with $A_{\|} = 135$ G and $g_{\|} = 2.36$, which is assigned to hydrated octahedrally coordinated Cu^{2+}. Therefore, deactivation of Cu/ZSM-5 is not due to loss of accessibility of active copper sites.

4.3. Dealumination of Cu/ZSM-5 Zeolite and Deactivation Model for Cu/ZSM-5 Catalyst

The results obtained in this study suggest that deactivation of a Cu/ZSM-5 catalyst is accompanied by dealumination of the zeolite support. In discussing a model for the deactivation process, the following results have to be taken into consideration. First, the TPR profile of Cu/ZSM-5-18-113 that has been reduced and reoxidized is very similar to that of a fresh sample (compare Fig. 3, curves a and b). Oxidation of copper to CuO, followed by protonolysis apparently leads to redispersion of copper (Scheme I).

$$Cu^0 \xrightarrow[200^\circ C]{1/2O_2} CuO \xrightarrow[500^\circ C]{2H^+/-H_2O} Cu^{2+}$$

SCHEME I

This type of chemistry has previously been demonstrated for Pd/Y (27) and Rh/Y (28). A requirement for protonolysis to take place is that the exchange sites of the zeolite remain available. In contrast, the TPR profile of deactivated Cu/ZSM-5-18-113 after reduction and reoxidation is very different from that of the original sample (compare Fig. 3, curves d and e). This suggests that either the exchange sites are no longer available or there are sites in the deactivated sample that interact more strongly with CuO than the zeolite exchange sites, so that redispersion of Cu^{2+} and its return to the exchange sites remains incomplete. Second, comparison of the catalytic activities and the TPR and EPR patterns of deactivated Cu/ZSM-5 with those of Cu/H-ZSM-5-ST indicates that dealumination of the zeolite support takes place. This implies permanent loss of ion-exchange sites and, consequently, irreversible changes of the state of the copper.

It appears that deactivation of Cu/ZSM-5 can be attributed to two major causes.

(a) Dealumination-induced deactivation: Even for a 116% exchanged Cu/ZSM-5, not all of the exchange sites are occupied by Cu^{2+} ions. Their hydrolysis generates zeolite protons (see Eq. [4]), and so does their reduction to Cu^+. The proton sites will be susceptible to dealumination by steaming, as they are in H-ZSM-5. This has been confirmed by Armor and Farris (29) who showed that Cu/ZSM-5 was dealuminated after exposure to 2% H_2O at 750°C, although much less severely than H/ZSM-5 treated under the same conditions. Grinsted *et al.* observed a similar result after treatment in 10% H_2O at 410°C (12). Their results showed that the loss of framework aluminum was almost equal to the percentage of unexchanged sites (H-sites) of the original ZSM-5. Steam-dealumination of H-ZSM-5 resulting in the formation of amorphous Al_2O_3 has been documented using ^{27}Al NMR (30).

Amorphous alumina formed inside ZSM-5 can react with Cu^{2+} on the exchange sites to form a stable CuO cluster on Al_2O_3 (Eq. [11]) or even a stoichiometric $CuAl_2O_4$ compound:

$$Cu^{2+}/[AlO_2^-]_2 + H_2O + Al_2O_3 \Longrightarrow CuO/Al_2O_3 + 2H^+/[AlO_2^-]. \quad [11]$$

Additional protons which will be susceptible to further dealumination are formed. It is concluded that simple steaming of Cu/ZSM-5 alone can result in irreversible deactivation. The strong interaction between Cu ions and γ-Al_2O_3, which leads to the formation of $CuAl_2O_4$, has been studied by Bolt *et al.* (31). They found that the rate of Cu incorporation into γ-Al_2O_3 was much faster than other ions studied, which included Fe, Ni, and Co. The diffusion of Cu into γ-Al_2O_3 can occur at temperatures as low as 500°C and is greatly accelerated in the presence of steam.

(b) Reaction-induced deactivation: A redox mechanism, involving valence changes of Cu^{2+} to Cu^+ under lean NO_x reduction condition, has been proposed (23, 32–34). For charge balance, reduction of Cu^{2+} to Cu^+ must be accompanied by formation of protons at the exchange site, making this site more susceptible to dealumination by steaming. In addition, complexing of Cu^{2+} ions by charged intermediates such as bidentate nitrate ions, isocyanate ions, etc., could also leave the exchange sites unprotected by Cu^{2+}, thus enhancing dealumination. That is, the lean NO_x reduction environment facilitates dealumination. This explains why the deactivation rate is much faster under the lean NO_x condition (standard wet condition) than under any other condition.

5. CONCLUSION

Deactivation of Cu/ZSM-5 under conditions of lean NO_x reduction with propane is faster than if any one of the feed component is lacking. Hydrolysis of Cu^{2+} ions to $[Cu–O–Cu]^{2+}$ oxocations and agglomeration to CuO particles implies formation of zeolite proton exchange sites. The proton exchange sites could also be formed under lean NO_x reduction conditions by Cu^{2+} reduction, or by displacement of Cu^{2+} ions from exchange sites when Cu^{2+} ions form complexes with negatively charged ligands such as nitrate or other ions. Exchange sites that have been vacated by Cu^{2+} and occupied by protons are susceptible to dealumination by steaming. Dealumination induces redistribution of Cu^{2+} ions as they interact rather strongly with the alumina clusters. Formation of highly dispersed copper on/in Al_2O_3 or copper aluminate results in Cu^{2+} ions in sites so dispersed that antiferromagnetic coupling with other Cu^{2+} ions is weak. Therefore, the number of Cu^{2+} ions detectable by EPR is higher in the deactivated than in the fresh catalyst. Interaction of some copper with the silicious portion of the dealuminated zeolite is not excluded, but no definite evidence has been obtained. In more severely deactivated and dealuminated Cu/ZSM-5 catalyst, the interaction of Cu with alumina appears to dominate.

ACKNOWLEDGMENTS

We thank B. J. Adelman for providing Cu/ZSM-5-18-113 sample, and S. Babitz for recording the ^{27}Al NMR spectra. Support of this work by the Ford Motor Corporation and the Engelhard Corporation is gratefully acknowledged.

REFERENCES

1. Iwamoto, M., and Hamada, H., *Catal. Today* **10**, 57 (1991).
2. Truex, T. J., Searles, R. A., and Sun, D. C., *Platinum Metals Rev.* **36**, 2 (1992).
3. Iwamoto, M., Yahiro, H., Shundo, S., Yu-U, Y., and Mizuno, N., *Shokubai (Catalyst)* **32**, 430 (1990).
4. Held, W., Konig, A., Rihter, T., and Ruppee, L., SAE Paper 900496 (1990).
5. Burch, R., and Scire, S., *Appl. Catal. B* **3**, 295 (1994).
6. Bethke, K. A., Alt, D., and Kung, M. C., *Catal. Lett.* **25**, 37 (1993).
7. Kung, M. C., Bethke, K. A., Alt, D., Yang, B., and Kung, H. H., "Reduction of Nitrogen Oxide Emissions," ACS Symposium Series 587, Chap. 8, 1995.
8. Kharas, K. C. C., Robota, H. J., and Liu, D. J., *Appl. Catal. B* **2**, 225 (1994).
9. Matsumoto, S., Yokata, K., Doi, H., Kimura, M., Sekizawa, K., and Kasahara, S., *Catal. Today* **22**, 127 (1994).
10. Petunchi, J. O., and Hall, W. K., *Appl. Catal. B* **3**, 239 (1994).
11. Grünert, W., Hayes, N. W., Joyner, R. W., Shpiro, E. S., Siddiqui, M. R. H., and Beava, G. N., *J. Phys. Chem.* **98**, 10832 (1994).
12. Grinsted, R. A., Zhen, H. W., Montreuil, C., Rokosz, M. J., Shelef, M., *Zeolite* **13**, 602 (1993).
13. Tabata, T., Kokitsu, M., Okada, O., Nakayama, T., Yasumatsu, T., and Sakane, H., Catalyst deactivation 1994, *in* "Studies in Surface Science and Catalysis" (B. Delmon and G. F. Froment, Eds.), Vol. 88, p. 409. Elsevier Science, Amsterdam, 1994.
14. Iwamoto, M., Yahiro, H., Mizuno, N., Zhang, W., Mine, Y., Furukawa, H., and Kagawa, S., *J. Phys. Chem.* **96**, 9360 (1992).
15. Hierl, R., Urbach, H. P., and Knözinger, H., *J. Chem. Soc. Faraday trans.* **88**(3), 355 (1992).
16. Bartholomew, C., Gopalakrishnan, R., Stafford, P. R., and Davison, J. E., AlChE 1992 Annual Meeting, Paper 240a.
17. Delk II, F. S., and Vevere, A., *J. Catal.* **85**, 380 (1984).
18. Spoto, G., Zecchina, A., Bordiga, S., Ricchiardi, G., and Martra, G., *Appl. Catal. B* **3**, 151 (1994).
19. Sárkány, J., d'Itri, J. L., and Sachtler, W. M. H., *Catal. Lett.* **16**, 241 (1992).
20. Lei, G.-D., Adelman, B. J., Sárkány, J., and Sachtler, W. M. H., *Appl. Catal. B* **5**, 245 (1995).
21. Valyon, J., and Hall, W. K., *J. Phys. Chem.* **97**, 7045 (1993).
22. Jacobs, P. A., Tielen, M., Linart, J. P., Uytterhoeven, J. B., and Beyer, H., *J. Chem. Soc. Faraday I* **72**, 2793 (1976).
23. Tanabe, S., and Matsumoto, H., *Appl. Catal.* **45**, 27 (1988).
24. Beutel, T., Sárkány, J., Lei, G.-D., Yan, J. Y., and Sachtler, W. M. H., *J. Phys. Chem.* in press.
25. Sachtler, W. M. H., and Zhang, Z., *Adv. Catal.* **39**, 129 (1993).
26. Homeyer, S. T., and Sachtler, W. M. H., *J. Catal.* **118**, 266 (1989).
27. Feeley, O. C., Sachtler, W. M. H., *Appl. Catal.* **75**, 93 (1991).
28. Tomczak, D. C., Schünemann, V., Lei, G.-D., and Sachtler, W. M. H., *Microporous Mater.,* in press.
29. Armor, J. N., and Farris, T. S., *Appl. Catal. B* **4**, L11 (1994).
30. Suzuki, K., Sano, T., Shoji, H., and Murakami, T., *Chem Lett.* 1507 (1987).
31. Bolt, H. P., "Transition Metal Aluminate Formation in Alumina-Supported Model Catalysts: High Energy Ion Beam Analysis of Interfacial Processes," Chaps. 5 and 6, Ph.D. thesis, University of Utrecht, Netherlands, 1994.
32. Liu, D. J., and Robota, H. J., *Appl. Catal. B* **4**, 155 (1994).
33. Li, Y., and Hall, W. K., *J. Catal.* **129**, 202 (1991).
34. Burch, R., and Millington, Y. J., *Appl. Catal. B* **2**, 101 (1993).